Journal of New Materials for Electrochemical Systems 21, 037-042 (2018)

Thermally Deposited Sb_2S_3: Bi Thin Films for Solar Cell Absorber

Durai Chella Priya[1], Thanabalan Daniel[1], Johnson Henry[1], Kannusamy Mohanraj[1,*], Ganesan Sivakumar[2], Sethuramachandran Thanikaikarasan[3] and Pathiyamattom Joseph Sebastian[4]

[1]Department of Physics, Manonmaniam Sundaranar University, Abishekapatti, Tirunelveli – 627 012, Tamil Nadu, India
[2]CISL, Department of Physics, Annamalai University, Chidambaram - 608 002, Tamil Nadu, India
[3]Centre for Scientific and Applied Research, School of Basic Engineering and Sciences, PSN College of Engineering and Technology, Tirunelveli – 627 152, Tamil Nadu, India
[4]Instituto de Energias Renovables, UNAM 62580, Temixco, Morelos, Mexico

Received: October 13, 2017, Accepted: December 20, 2017, Available online: April 17, 2018

Abstract: *In recent years there has been growing interest in the materials suitable for real time storage application. Sb_2S_3 is a prospective material in this regard due to good photoconductivity. In this contest, thin films of Sb_2S_3 and Bi^{3+} doped Sb_2S_3 were deposited onto the transparent glass substrate by thermal evaporation method. The structural, optical and electrical properties were investigated by XRD, UV-Visible, Photoluminescence, and Impedance spectroscopic techniques. The XRD patterns confirm the orthorhombic crystal structured Sb_2S_3 and the inclusion of Bi^{3+} ions in the crystal system. UV-Visible analysis exhibited wide optical absorption in the visible region for both Sb_2S_3 and Bi^{3+} doped films and their band gap energy was found to be 1.60 eV and 1.55 eV respectively. The photoluminescence spectra showed a strong emission at 361nm. The value of capacitance, dielectric constant and real part of impedance decreases with increasing frequency for both the samples.*

Keywords: antimony sulfide, bismuth, thin film, dielectric

1. INTRODUCTION

Binary and ternary chalcogenides of Sb_2S_3 are promising materials for electronic devices applications especially in photoconductive target for the videocon type of television camera tubes, microwave, switching and optoelectronic devices. Sb_2S_3 thin films are used in solar energy conversion and thermoelectric cooling technologies [1] among the available chalcogenides. Sb_2S_3 has attracted much attention due its unique properties such as high optical absorption coefficient, optimum band gap (Eg = 1.8 eV), high refractive index, well-defined quantum size effects, this material exhibit structural modification when irradiated by light and by an electron beam, their photosensitive and thermoelectric properties. There is a number of reports on the structural and optical properties of Sb_2S_3 thin films prepared by various techniques such as spray pyrolysis [2], Thermal evaporation [3], chemical bath deposition method [4]. Among the deposition method, the thermal vacuum evaporation technique is relatively simple method to prepare homogeneous Sb_2S_3 thin films. Extensive research has been done on the deposition and characterization of Sb_2S_3 semiconducting thin films due to their potential application in the area of optoelectronic device fabrication and microwave. Sb_2S_3 thin films have good optical transmittance, wide band gap and electrical properties suitable for their application to solar cell fabrication [5]. The properties of Sb_2S_3 can be tuned for desired applications. Doping is the suitable way to tune the physical properties of Sb_2S_3 thin films. S.S. Salim et al., 2010 prepared Ag doped Sb_2S_3 thin films and observed decrease in band gap with increase in Ag concentration [6]. N. J. Mathew et al., 2011 studied the dielectrical and impedience properties of Se doped Sb_2S_3 thin films and found that the bandgap increases with increase in doping [7]. S. Muataq et al., 2016 studied the optical properties of Ni doped Sb_2S_3 thin films and Sn doped Sb_2S_3 thin films found that the bandgap energy increases with increase in doping concentration [8, 9]. E. Ca´ rdenas

*To whom correspondence should be addressed:
Email: kmohanraj.msu@gmail.com; mohanraj@msuniv.ac.in

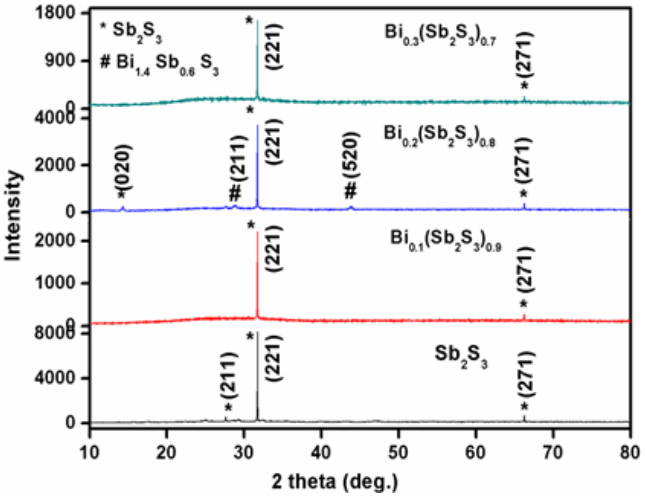

Figure 1. XRD patterns of Sb_2S_3 and Bi doped Sb_2S_3 thin films

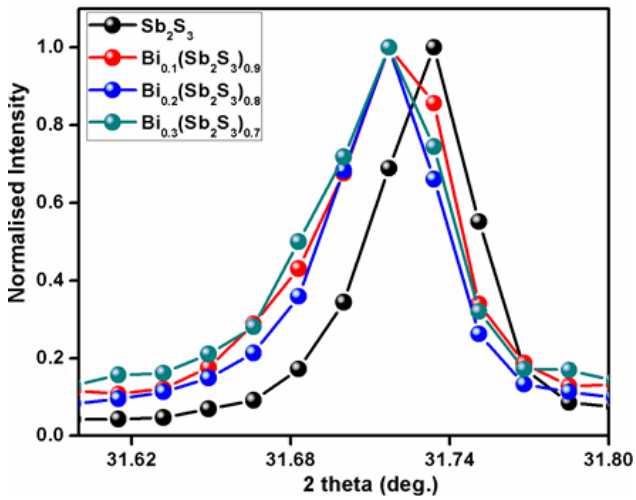

Figure 2. Peak shift of Sb_2S_3 and Bi doped Sb_2S_3 thin films

et al., 2009 studied the electrical properties of Carbon doped Sb_2S_3 thin films [10]. Hence it is noticed that the doping of metals in Sb_2S_3 thin films tunes the optical and electrical materials of the Sb_2S_3 thin films. Also it is noticed that Bi doped Sb_2S_3 thin films not explored well elsewhere. Therefore, it is motivating to prepare pure Sb_2S_3 and Bi doped Sb_2S_3 thin films by thermal vacuum evaporation technique and to study its opto structural characteristics.

2. EXPERIMENTAL DETAILS

Microscopic glass slides size (76 mm x 26 mm x 1.15 mm) was cleaned well with chromic and then the slides were cleaned with detergent solution. The substrates was adopted by the earlier report [11]. The substrates were once again washed by distilled water and then dried in air. AR grade of antimony sulfide (99.999% purity) and Bismuth (99.999% purity) was purchased from the Merch company were used as starting materials. Antimony sulfide (90 % wt ratio) and bismuth powder (10 % wt ratio) was pelletized by applying 5 ton of pressure using hydrolyic press. The pellet was kept in the molybdenum boat. Prior to evaporation, the pellet was carefully degassed at lower temperature for 45 minutes. The current supply was slowly increased and maintained 90 amp for complete evaporation of the sample. The pressure inside the champer was maintained about $2x10^{-5}$ Torr. A similar process was adopted for the preparation of $(Bi)_x(Sb_2S_3)_{1-x}$thin films (x=0.1; 0.2; 0.3). The Bi doped Sb_2S_3 thin films were brown in colour. The deposited films were anealed at 250°C for 1 h in air atmosphere. the thickness of the film was calculated by using the standard procedure [6].

The structural characteristics were carried out by analyzing the XRD patterns obtained using CuKα radiation (λ=1. 5406Å) in an X'pert PRO X- ray diffractometer. The optical measurements were performed using Hitachi U3400 UV- Vis spectrometer. The photoluminescence spectra measurements are carried out by using PERKIN ELMER LS45. Dielectric measurements were taken for the thin films in the frequency range from 50 Hz – 5 MHz by using impedance analyser using CH instruments CHI60E electrochemical analyzer.

3. RESULTS AND DISCUSSION

Figure 1 shows the XRD patterns Sb_2S_3 and Bi doped Sb_2S_3 films of annealed at 250° C for 1 hr. In Fig.1, a crystalline peaks observed at d-spacing 2.7646A° and 1.4397A° corresponding to (221) and (271) planes respectively of orthorhombic structured Sb_2S_3. The diffraction peaks are well matched with the standard Sb_2S_3 [JCPDS card no: 06-0474] and similar results were reported for the Sb_2S_3 [3, 12].

Fig 1 (b-d) represents the XRD patterns of Bi doped Sb_2S_3 thin films. The intensity of the plane (221) is decreased with increase in Bi concentration which indicates the deterioration in the film property. When introducing Bi into Sb_2S_3 pattern due to the strain produced in the lattice. These observations confirm the incorporation of Bi atoms in the lattice structure of Sb_2S_3. The observed peaks at 66.24° corresponding to the plane (5 2 2) orthorhombic structured $Bi_{1.4}Sb_{0.6}$ S_3 (JCPDS Card No 361229). The $Bi_{1.4}$ $Sb_{0.6}$ S_3 peaks in the XRD results confirm the blend of Bi into Sb_2S_3.

The diffraction result also reveals that the incorporation of Bi^{3+} ions does not change the crystal structure of the Sb_2S_3 host lattice . Since, the ionic radius of Bi^{3+} (1.17Å) is larger than that of Sb^{3+} (0.90 Å), it is impossible for Bi^{3+} to act as interstitial ions in the Sb_2S_3 host matrix. The Bi^{+} can only replace Sb^{3+} substitutionally in the Sb_2S_3 lattice sites. Figure 2 shows the peak shift of plane (221) toward the lower angle because the ionic radius of Bi^{3+} (1.17Å) is higher than that of Sb^{3+} (0.90 Å).

The average crystallite size and micro structural parameters such as dislocation density (δ) and micro strain (ε) of undoped Sb_2S_3 and Bi doped Sb_2S_3 were calculated using the following equations. Debye – Scherrer relation equation as follows [13].

$$D = K\lambda / \beta c\cos\theta \quad (1)$$

Where, D_{hkl} is the mean grain size of ordered (crystalline) domains(nm), λ is the wavelength of characteristics X rays (Å), θ is the bragg diffraction angle of the respective diffraction peak, β is the full width at half maximum of the peak and K varies with (h k l) and crystallite shape but usually equal to 0.94.

Dislocation Density (δ) and Micro Strain (ε) can be calculated by

UNCORRECTED PROOF

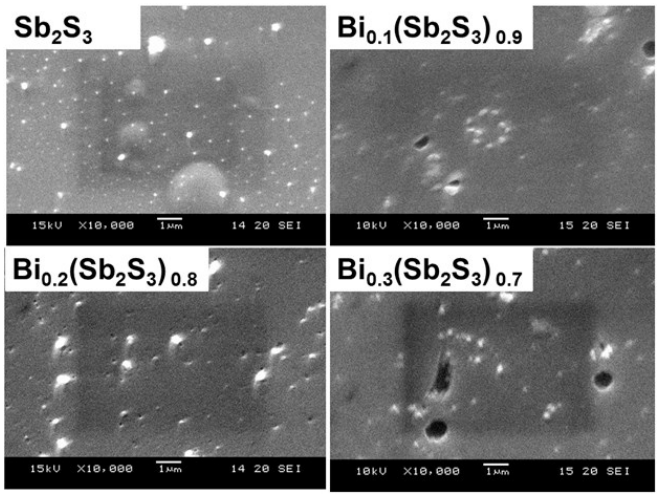

Figure 3. SEM images of pure and Bi doped Sb_2S_3 thin films

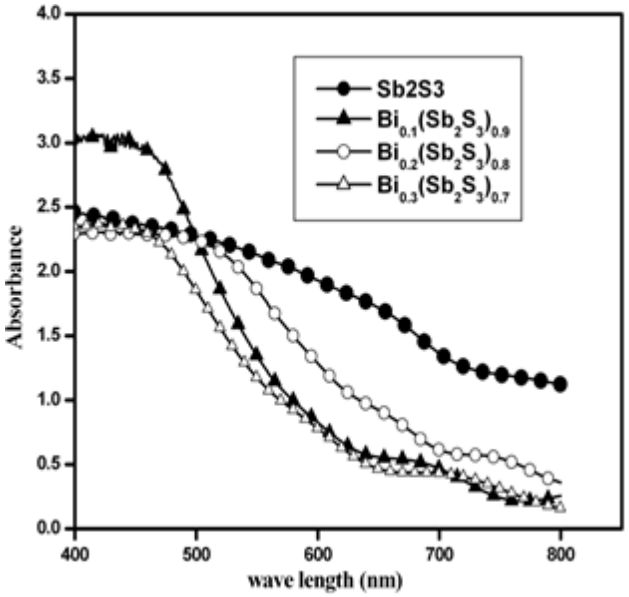

Figure 4. Absorption spectra of Sb_2S_3 and Bi doped Sb_2S_3 thin films

the following formula [14, 15]

$$\delta = 1/D^2 \quad (2)$$

$$\varepsilon = (\beta c \cos\theta)/4 \quad (3)$$

From the table it is found that the crystallite size increases with increase in doping except for 0.3% Bi concentration. This decrease in crystallite size for 0.3Bi doping may be caused by the enhanced incorporation of Bi^{3+} ions into the Sb^{3+} sites of the host Sb_2S_3 lattice. The decrease of crystallite size means deteroriation of crystalline quality of Sb_2S_3 films with Bi doping and an increase of total grain boundary fraction in the films, which can enhance grain boundary scattering, thus, result in an increase of electrical resistivity [16].

Figure 3 shows the SEM images of pure and Bi doped Sb_2S_3 thin films. From the figure it is found that the films are uniform and smooth surface.

Figure.4 shows the optical absorption spectra of Sb_2S_3 and Bi doped Sb_2S_3 thin films. The Sb_2S_3 thin film showed wide band of absorbance within the visible region while. Bi doped Sb_2S_3 sample has higher absorbance between 400 – 500 nm. The spectra also showed a gradually increasing absorbance throughout the visible region, which makes it possible for this material to be used in a photo electrochemical cells. Doping content reduces the broadness of the peak, may be due to the rearrangement of ions into lattice. From the absorbance spectra, the absorption coefficient (α) at each energy ($h\nu$) can be evaluated. The optical absorption studies are very useful to identify the band gap, refractive index, extinction coefficient etc. The absorption coefficient is calculated from the relation equation (1).

$$\alpha = 2.303/t \log 1/T \quad (4)$$

where, α is the absorption coefficient, t is the thickness of the thin film, T is the transmittance of the material. The absorption coefficient α is related to the energy gap Eg according to the Tauc equation (5)[7],

$$(\alpha h\nu) = A(h\nu - E_g)^n \quad (5)$$

where, A is a constant that depends on the transition probability, h is the planck constant and n is equals ½ for direct band gap. The high absorbance exhibited by this material makes it a potential absorber material in devices for photovoltaic conversion of solar energy. The absorption coefficient was found to be about 10^5 cm^{-1} and it is well agreed with the earlier reports on amorphous Sb2S3 thin films prepared by vacuum evaporation method [17].

The band gap E_g was determined by extrapolating the linear portion of the $(\alpha h\nu)^2$ vs $h\nu$ curve to intercept the horizontal photon energy axis as shown in Fig.5. The energy gap values of Sb_2S_3 thin

Table 1. Crystallite size, dislocation density, micro strain and thickness of the prepared films

Sample	Crystallite size (nm)	Micro strain	Dislocation Density ($x10^{14}$ lines/m^2)	Thickness (μm)
Sb_2S_3	84	6×10^{-4}	1.417	15.3
$Bi_{0.1}(Sb_2S_3)_{0.9}$	97	3×10^{-4}	1.0628	3.4
$Bi_{0.2}(Sb_2S_3)_{0.8}$	129	7×10^{-4}	1.6866	4.1
$Bi_{0.3}(Sb_2S_3)_{0.7}$	77	3×10^{-4}	0.6009	6.6

UNCORRECTED PROOF

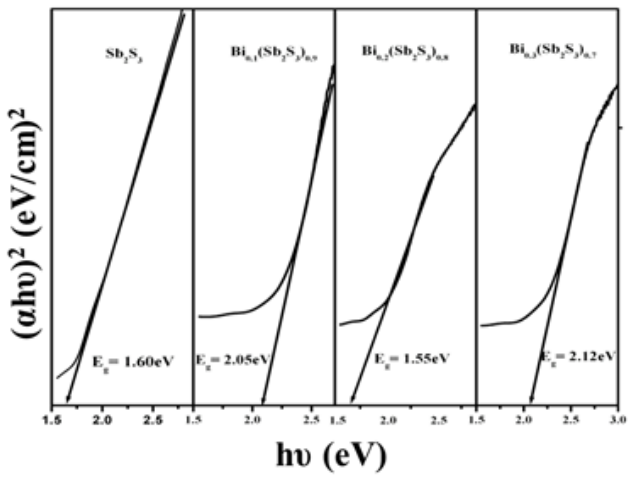

Figure 5. Band gap energy of Sb_2S_3 and Bi doped Sb_2S_3 thin films

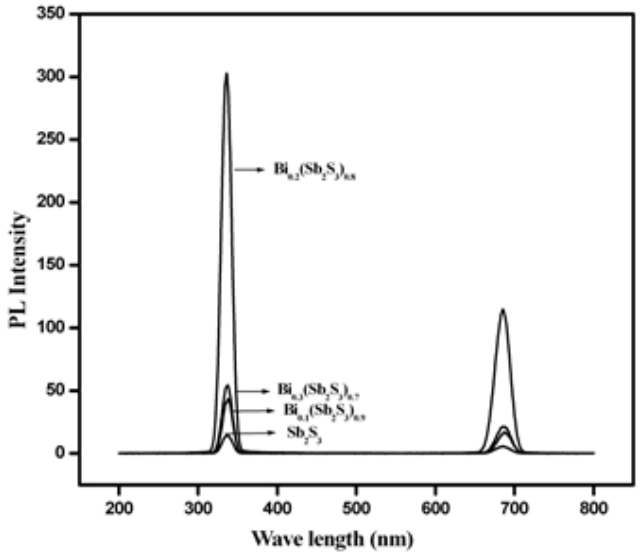

Figure 6. Photoluminescence Spectra of Sb_2S_3 and Bi doped Sb_2S_3 thin films

film is found to be E_g = 1.60 eV and E_g = 1.55 eV – 2.12 eV for Bi doped Sb_2S_3 respectively. The lower band gap energy in Sb_2S_3 is due to smaller thickness and certain size effects like quantum size effect may arise in the film [18]. The result is in good agreement with the Sb_2S_3 thin films prepared by vacuum evaporation and chemical bath deposition methods [19, 20].

A consequence of quantization in the energy spectrum, the bottom of the conduction and top of the valence band may be separated by additional amount depending on thickness. The uppermost occupied valence band and lowest occupied conduction band are shifted to more negative and positive values respectively resulting in broaden of the band gap. The addition of Bi in Sb_2S_3 crystal lattice causes size differences. It may create new coordination and variation in the bonding and orbital contributions toward valence and conduction bands. Hence the addition of Bi introduces change

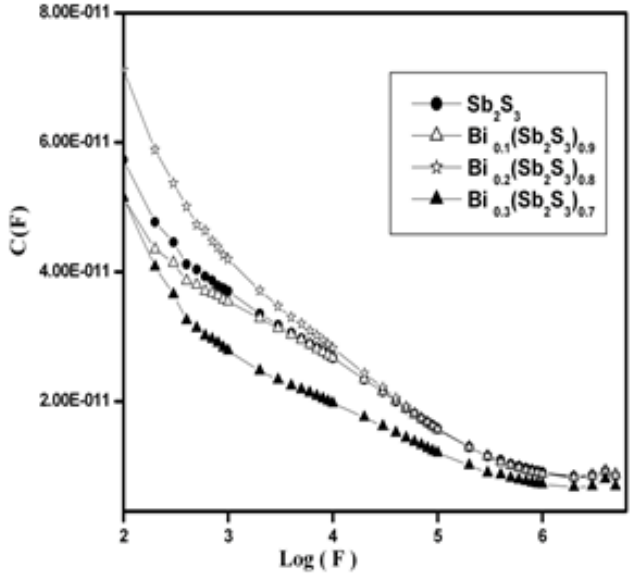

Figure 7. Variation of capacitance with frequency

in band gap.

Incorporation of Bi into Sb_2S_3 is confirmed using XRD and the structural changes reflected in UV –Vis and PL studies.

The photoluminescence technique has been widely used to investigate the energy levels of thin films. Fig.6 shows the photoluminescence spectra of Sb_2S_3 and Bi doped Sb_2S_3 thin films. The dominant sharp emission is noticed peak at 335 nm for all the films attributed to photon assisted transitions and electron-hole recombination after relaxation (band edge emission). This results is in close agreement with the report by F.Capezutto et al.,[21]. The weak emission peak at 686 nm is due to the emission from the recombination of electrons and holes in trapped surface states located in the forbidden region of the band gap. The increase in photoluminescence intensity in 0.2% Bi is due to crystalline size because PL intensity is reciprocal of the square of the crystallite size [21]. All the emission are associate with defects emerging during the growth of crystallites and are related to deformation of crystallinity due to dislocations and large vacancies.

The dielectric constant is the result of the contribution of several kinds of polarizations as deformational (electronic, ionic) as well as relaxation (orientational and interfacial). When the frequency is increased, the electric dipoles cannot follow the field which leads to the decrease of orientation polarization. At high frequency, ε reached a constant value due to interfacial polarization. Fig.7 shows the variation of capacitance with frequency for undoped Sb_2S_3 and 0. 1%, 0.2%, and 0.3% Bi doped Sb_2S_3 thin films in the frequency range 50 Hz to 5 MHz. The capacitance decreases with increasing frequency and attain a constant value at higher frequencies.

The variation of dielectric constant (ε) with frequency for the undoped Sb_2S_3 and 0. 1%, 0.2%, and 0.3% Bi doped Sb_2S_3 thin films is presented in Fig.8. The dielectric constant decreases with increasing frequency. This decrease may be due to fact the orientational polarization decreases when the frequency is increased. The value of dielectric constant attains a constant value at higher fre-

UNCORRECTED PROOF

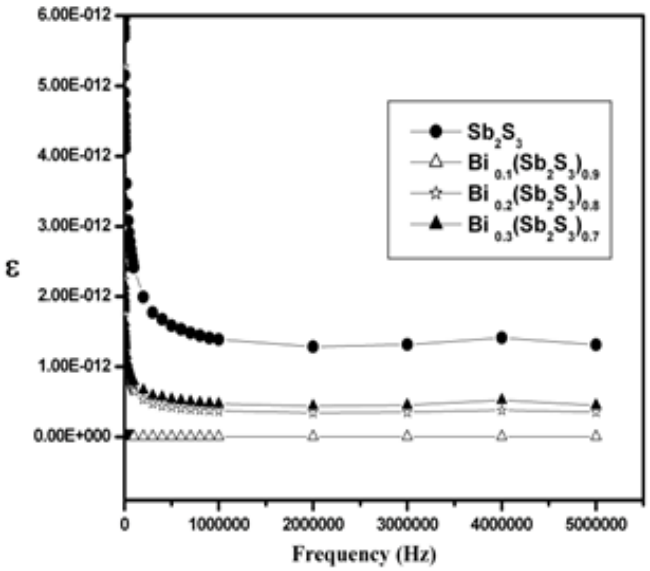

Figure 8. Variation of dielectric constant with frequency

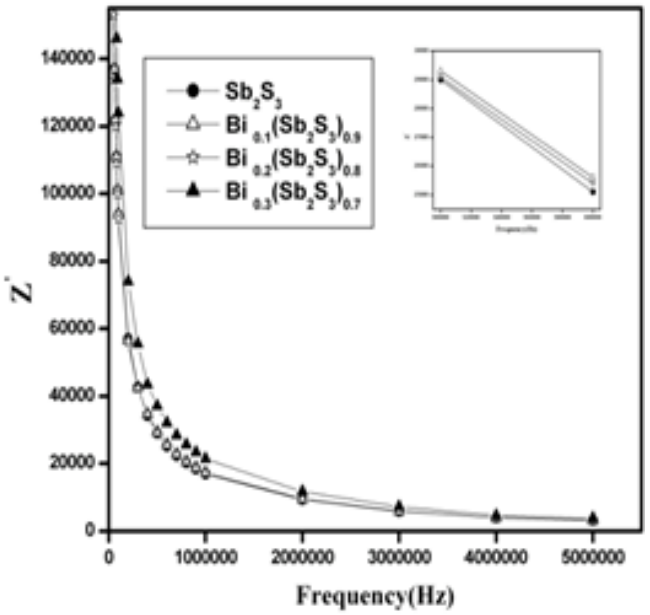

Figure 9. Variation of impedance (Z') with frequency

quency due to interfacial polarization. The variation of real part of impedance (Z') with the frequency for the of pure Sb_2S_3 and 0. 1%, 0.2%, and 0.3% Bi doped Sb_2S_3 thin films is shown in fig.9. It is clear from the magnitude of Z' decreases with the increase of frequency. This result is in agreement with the reported results published by N.Jessy Mathew et al., [7].

4. CONCLUSIONS

Sb_2S_3 and Bi-Sb_2S_3 thin films were successfully prepared by thermal evaporation technique. The deposited films were annealed at 250 °C and were characterized by using XRD, UV-Visible and Photoluminescence analysis. The XRD analysis confirms the orthorhombic structure of Sb_2S_3 thin films. The incorporation of Bi into the Sb_2S_3 lattice leads to prominent peak shift towards the lower angle. UV-Visible analysis shows Bi doped Sb_2S_3 thin films having higher optical absorption in the visible region than that of pure Sb_2S_3 thin films. 0.2 % of Bi doped Sb_2S_3 thin film shows increased PL intensity compared to all other thin films due to the lower crystallite size. The value of capacitance, dielectric constant and real part of impedance decreases with increasing frequency for both the samples.

5. ACKNOLOWDGEMENT

The authors are thankful to the UGC-SAP, New Delhi for providing the financial support to the Department of Physics, Manonmaniam Sundaranar University, Tirunelveli, Tamil Nadu, India.

REFERENCE

[1] F. Aousgi, M. Kanzari, Current Applied Physics, 13, 262, (2013).
[2] S. Srikanth, N. Suriyanarayanan, S. Prabahar, V. Balasubramanian, D. Kathirvel, Opto Electronics and Advanced Materials-Rapid Communications, 4, 2057, (2010).
[3] N. Tigau, V. Ciupina, G. Prodan, G. I. Rusu, C. Gheorghies, E. Vasile, Journal of Optoelectronics and Advanced Materials 6, 211, (2004).
[4] A.U. Ubale, V.P. Deshpande, Y.P. Shinde, D.P. Gulwade, chalcogenide letter 7, 101, (2010).
[5] N. Tigau, V. Ciupina, G. I. Rusu, G. Prodan, E. Vasile, Rom. J. Phys, 50, 859, (2005).
[6] Siham. M. Salim, M.B. Seddek, A.M. Salem and Islam, Journal of Applied Science Research, 6, 1352, (2010).
[7] N.J. Mathew, R. Oommen, P.U. Rajalakshmi, C. Sanjeeviraja, Chalcogenide Letters 8, 441, (2011).
[8] Saima Mushtaq, Bushra Ismail, Muhammad Raheel, Aurang Zeb, Natural Science, 8, 33, (2016).
[9] Saima Mushtaq, Bushra Ismail, Misbah Aurang Zeb, N.J. Suthan Kissinger, Aurang Zeb, Journal of Alloys and Compounds, 632, 723, (2015).
[10]Emma Cardenas, A. Arato, E. Perez-Tijerina, T.K. DasRoy, G. AlanCastillo, B. Krishnan, Solar Energy Materials & Solar Cells, 93, 33, (2009).
[11]Nordin Sabli, Zainal Abidin Talib, Wan Mahmood Mat Yunus, Zulkarnain Zainal, Hikmat S. Hilal, Masatoshi Fujii, Materials Science Forum, 756, 273, (2013).
[12]R. Oommen, N.J. Mathew, P.U. Rajalakshmi, Journal Of Ovonic Research, 6, 259, (2010).
[13]N. Tigau, Rom, J..Phys. 53, 209, (2008).
[14]Subhash Chander, M.S. Dhaka, Adv. Mater. Lett., 6(10), 907, (2015).
[15]Salah Abdul-Jabbar Jassim, Abubaker A. Rashid Ali Zumaila, Gassan Abdella Ali Al Waly, Results in Physics, 3, 173, (2013).
[16]N. Manjula, M. Pugalenthi, V.S. Nagarethinam, K. Usharani,

A.R. Balu, Materials Science-Poland, 33(4), 774, (2015).
[17]F. Aousgi, M. Kanzari, Journal of Optoelectronics and Advanced Materials, 12, 227, (2010).
[18]B. Ismail, S. Mushtaq, R. A. Khan, A. M. Khan, A. Zeb, A. R. Khan, Optik - International Journal for Light and Electron Optics, 125, 6418, (2014).
[19]N. Tigau, Cryst.Res. Technol., 42, 281, (2007).
[20]P.U. Asogwa, S.C. Ezugwu, F.I. Ezema, R.U. Osuji, Chalcogenide Letters, 6, 287, (2009).
[21]F. Capezzuto, G. Carotenuto, F. Antolini, E. Burresi, M. Palomba, P. Perlo, Express Polymer Letters, 3, 219, (2009).